ELSEVIER

Materials Science and Engineering A273–275 (1999) 320–325

MATERIALS SCIENCE & ENGINEERING A

www.elsevier.com/locate/msea

Large field-induced strains in ferromagnetic shape memory materials

Richard D. James [a,*], Robert Tickle [a], Manfred Wuttig [b]

[a] *Department of Aerospace Engineering and Mechanics, University of Minnesota, Minneapolis, MN, 55455, USA*
[b] *Department of Materials and Nuclear Engineering, University of Maryland, College Park, MD 20742-2115, USA*

Abstract

We study magnetostriction in ferromagnetic shape memory materials caused by a redistribution of twin bands in response to an applied magnetic field. Recent measurements of strain versus magnetic field in Ni-24 at% Mn-24.7 at% Ga are presented. We report strains of about 0.5% under cyclic application of a field, and field-induced strains of about 4% on specimens that have been previously cooled through the martensitic transformation under stress. A comparison between these measurements and theoretical calculations reveals a discrepancy. We hypothesize that this is due to magnetization rotation, accompanied by the formation of fine magnetic domains within each band of martensite.

Keywords: Martensite; Magnetostriction

1. Introduction

Magnetostriction is the spontaneous deformation of a material caused by a change of its state of magnetization. In this paper we collect several recent measurements on the magnetomechanical behavior of $Ni_2Mn_xGa_{1-x}$ alloys that shed light on its magnetomechanical properties. Our particular interest here is the production of large reversible strains in martensites by the application of a modest magnetic field.

There are at least two ways of inducing large strains in ferromagnetic martensites. The first method typically requires that the saturation magnetization of the martensite differs from that of austenite. Depending on which phase has larger saturation magnetization, a field applied either above or below the martensitic transformation temperature will induce a transformation between austenite and martensite. Ignoring hysteresis and demagnetization effects, this phenomenon is governed by an appropriate version of the Clausius–Clapeyron equation, much like stress-induced transformation.

The second method involves the redistribution of martensite variants by an applied field at a fixed temperature below M_f, studied in detail by James and Wuttig [1] and Tickle et al. [2], and the subject of this paper. This case relies on the martensite being of low symmetry and therefore having a single easy axis. That is, the magnetization $\mathbf{m}$ in variant 1 of martensite, say, has an equal preference for the two values $\pm\mathbf{m}_1$, where $\mathbf{m}_1$ is crystallographic. The variants of martensite will generally have different easy axes $\mathbf{m}_1,\ldots,\mathbf{m}_k$, related to the easy axis of variant 1 by $\mathbf{m}_i = \mathbf{Q}\mathbf{m}_1$, where the Bain stretch matrices are correspondingly related by $\mathbf{U}_i = \mathbf{Q}\mathbf{U}_1\mathbf{Q}^T$. Since the total energy density contains a term $-\mathbf{h}\cdot\mathbf{m}$, where $\mathbf{h}$ is the applied field, then different applied fields will generally favor different variants of martensite. By competing one field against another, or a field against an appropriate stress, the minimum energy state can be made to shift from one variant to another leading to a change of shape.

For the second method it is important that the material have high magnetocrystalline anisotropy. That is, it must be difficult for an applied field to rotate the magnetization in variant 1 away from $\mathbf{m}_1$; this difficulty is quantified by magnetocrystalline anisotropy constants. For this reason the present strategy for producing large magnetostriction in martensites is almost exactly opposite to the idea employed by Clark and his co-workers [3–5] to discover the giant magnetostrictive material $Tb_xDy_{1-x}Fe_2$ ($x = 0.27$). Clark in fact sought

* Corresponding author. Tel.: +1-612-6250706; fax: +1-612-6261558.
E-mail address: james@aem.umn.edu (R.D. James)

0921-5093/99/$ - see front matter
PII: S0921-5093(99)00364-0

to achieve *low* effective anisotropy by adjusting x so that the material nearly had an ambiguous easy axis ([111] or [100]), at the confluence of two different magnetic phases. This general idea is also familiar to workers in martensite. In this way Clark obtained a material that had low hysteresis, and the naturally large magnetostrictive effect in the material could be accessed by a modest field. But an equally familiar idea to workers in martensite is the idea that high anisotropy in some cases is quite compatible with mobile twin boundaries. This underlies the strategy explored here: the high magnetocrystalline anisotropy keeps the magnetization near the easy axes, and the term $-\mathbf{h}\cdot\mathbf{m}$ therefore promotes a redistribution of mobile variants.

Given that the magnetization stays on the easy axis, except on transition layers that are analogous to the austenite/martensite interface, a greatly simplified theory can be formulated (DeSimone and James, [6]) called the *constrained theory*. This theory gives predictions of strain vs. field and corresponding microstructures for ferromagnetic martensites, based only on fundamental data (symmetries of parent and product, Bain strains, saturation magnetizations and easy axes). When this is compared to measurements of strain versus field in Ni-24 at% Mn-24.7 at% Ga (Tickle et al. [2]) good qualitative agreement, but significant quantitative disagreement, is found. A comparison is shown in Fig. 1. We believe that the disagreement is due to partial magnetization rotation and we suggest a possible mechanism in Section 3. This mechanism also shows that magnetocrystalline anisotropy is not the only property that affects rotation of magnetization.

The plan of this paper is as follows. Section 2 contains measurements of strain versus field and the aforementioned comparison between theory and experiment. It also shows the largest reversible field-induced strain that has been observed in ferromagnetic martensites: 4% in Ni-24 at% Mn-24.7 at% Ga at 12KOe, some 40 times the strain observed in giant magnetostrictive materials. Section 3 gives a mechanism for magnetization rotation within martensite bands suggested by magnetic force microscopy (MFM).

2. Field-induced redistribution of martensitic variants

The measurements reported in this section were performed on a single crystal specimen with composition Ni-24 at% Mn-24.7 at% Ga dimensions $8.4 \times 2 \times 2$ mm, and with faces normal to {100}. Strains were measured using an axial strain gage or by a visual method described below. The temperature was fixed at 256°K which is below the observed $M_f = 265$°K for this alloy.

The lower graph of Fig. 1 shows a typical measurement of strain versus field under cyclic application of

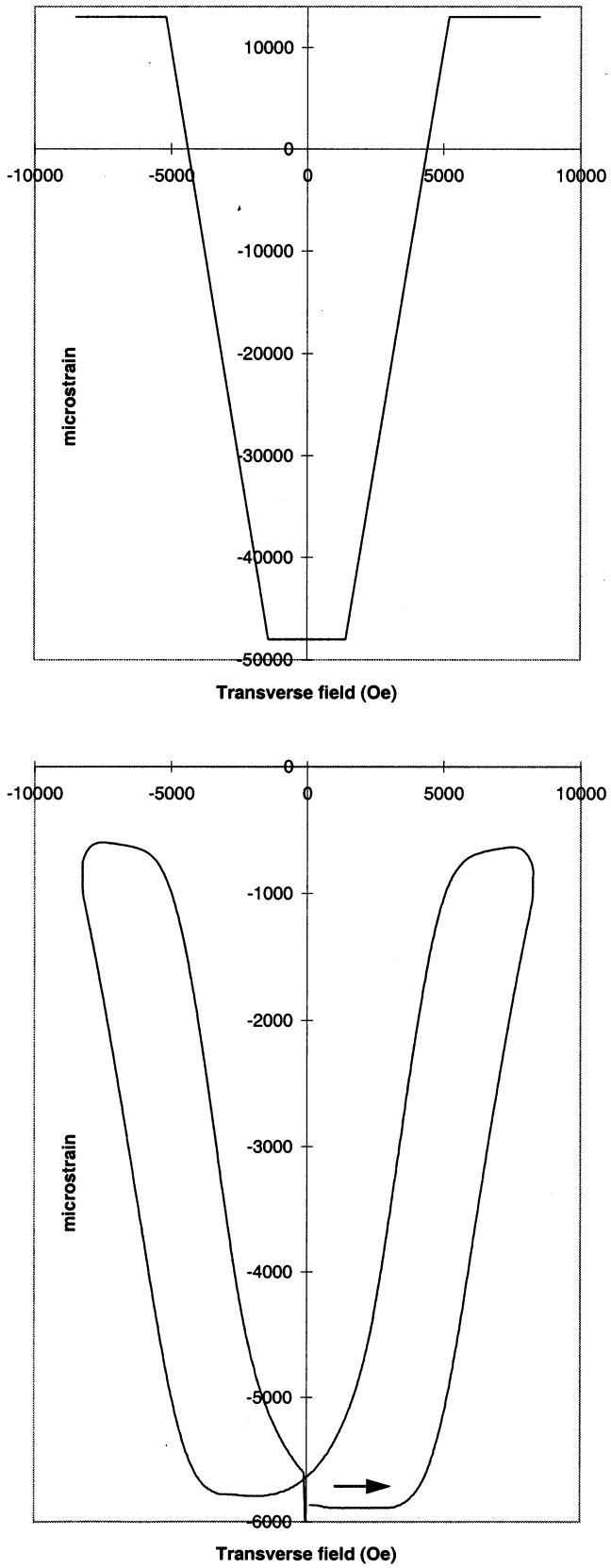

Fig. 1. Strain versus field in $Ni_{51.3}Mn_{24.0}Ga_{24.7}$. Transverse field applied along [010]. Upper: prediction of the constrained theory. Lower: experiment.

the field at about 0.2 Hz with amplitude of 8KOe. In this case the specimen is loaded by a constant 1.4 MPa compressive stress. The upper graph shows the prediction of the constrained theory under the corresponding conditions. This prediction is obtained by minimizing the constrained energy,

$$e(\mathbf{E}, \mathbf{m}) = \int_{\Omega} \{ -\mathbf{h} \cdot \mathbf{m}(\mathbf{x}) - \boldsymbol{\sigma} \cdot \mathbf{E}(\mathbf{x}) \} d\mathbf{x} + \frac{1}{8\pi} \int_{\mathbf{R}^3} |\nabla \zeta_m|^2 \, d\mathbf{x} \quad (2.1)$$

over all pairs of $(\mathbf{E}(\mathbf{x}), \mathbf{m}(\mathbf{x}))$, $\mathbf{x} \in \boldsymbol{\Omega}$, that belong to the energy wells $(\mathbf{E}_1, \pm \mathbf{m}_1)$, $(\mathbf{E}_2, \pm \mathbf{m}_2)$, $(\mathbf{E}_3, \pm \mathbf{m}_3)$, where

$$\mathbf{E}_1 = \begin{pmatrix} \epsilon_2 & & \\ & \epsilon_1 & \\ & & \epsilon_1 \end{pmatrix}, \quad \mathbf{m}_1 = \mathbf{m}_s[100],$$

$$\mathbf{E}_2 = \begin{pmatrix} \epsilon_1 & & \\ & \epsilon_2 & \\ & & \epsilon_1 \end{pmatrix}, \quad \mathbf{m}_2 = \mathbf{m}_s[010],$$

$$\mathbf{E}_3 = \begin{pmatrix} \epsilon_1 & & \\ & \epsilon_1 & \\ & & \epsilon_2 \end{pmatrix}, \quad \mathbf{m}_3 = \mathbf{m}_s[001], \quad (2.2)$$

with $\epsilon_1 = 0.013$, $\epsilon_2 = -0.048$, and $m_s = 602$ emu/cm^3 chosen for Ni-24 at% Mn-24.7 at% Ga. The applied stress is $\sigma = \text{diag}(-1.4 \text{ MPa}, 0, 0)$, and the applied field has the form $\mathbf{h} = (0, h, 0)$. For each applied field h in the interval (-8KOe, 8KOe), the total energy (2.1) is minimized. In (2.1) Ω is the region occupied by the specimen and ζ_m is the magnetostatic potential; it is determined from $\mathbf{m}(\mathbf{x})$ by solving $\text{div}(-\nabla\zeta_m + 4\pi\mathbf{m}) = 0$. Usually the minimizers exhibit microstructure, i.e., they are actually described by minimizing sequences $(\mathbf{E}^{(j)}(\mathbf{x}), \mathbf{m}^{(j)}(\mathbf{x}))$, $j = 1, 2, 3, \ldots$ having transition layers where the constraints (2.2) are not satisfied, but the total volume of these transition layers goes to zero as j tends to infinity. Physically, $1/j$ can be interpreted as domain wall thickness divided by a typical specimen size. The minimization procedure automatically takes care of this possibility, which is essential to treat mechanical or magnetic microstructures analogous to the austenite/martensite interface. From each of these minimizers (or minimizing sequences) the total axial strain (resp., limiting total axial strain) is calculated by integration.

Notice that there is a similarity between the two curves shown in Fig. 1, but the theory greatly overpredicts the strain. Similarly, there is qualitative agreement between the observed microstructures and the predicted ones, i.e. the variants and interfaces present agree well, but the predicted microstructures show a significantly greater change of volume fraction than the observed ones. A similar situation is found with a variety of applied fields (including different directions) and applied stresses (See Tickle et al. [2]). We return to this point in Section 3.

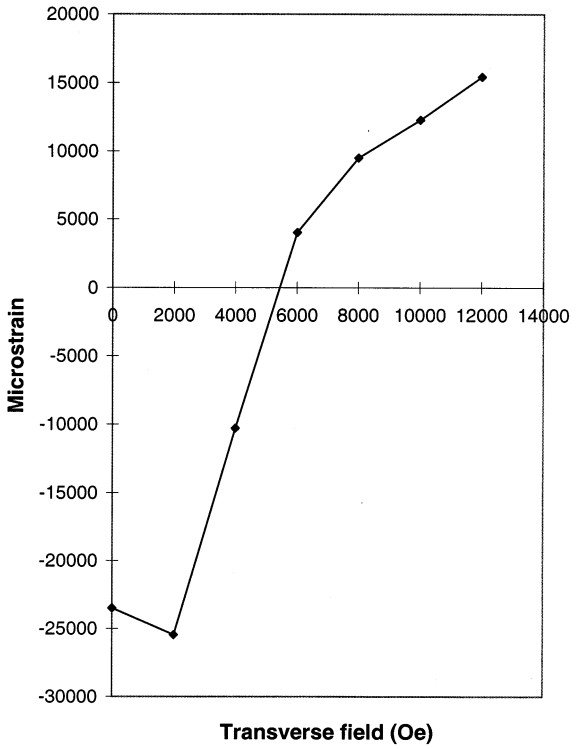

Fig. 2. Strain versus field measured after cooling through the austenite-martensite transformation under 2 MPa stress.

However, *if the initial state is set properly* by previously cooling through the austenite–martensite phase transformation under stress, the quantitative behavior predicted by the theory is obtained from measurements. Fig. 2 shows strain vs. field on the same specimen as above (but shortened to 4.3 mm) after cooling through M_f under an axial compressive stress of 2 MPa (The stress was removed before the measurement was performed). The strain here was measured using an optical microscope mounted on a stage equipped with an LVDT. Note that strains of approximately 4% are observed, corresponding to a volume fraction change of 0.625. This measurement is reproducible: by heating to above A_f and then repeating the test, we observed similar behavior. A photograph of the observed microstructure at three different fields is shown in Fig. 3.

3. The competition between variant rearrangement and magnetization rotation

There is nothing unusual about the martensitic microstructures observed during the tests, except that in some cases the volume fraction does not undergo the predicted large change. So, our attention is turned to

the magnetic behavior and particularly the possibility of magnetization rotation. If the magnetization rotates away from the easy axes during a test, the influence of the term $-\mathbf{h}\cdot\mathbf{m}$ on the different variants of martensite can be greatly diminished. In the extreme case that the magnetization in neighboring variants of martensite rotates so much that it becomes unidirectional, the term $-\mathbf{h}\cdot\mathbf{m}$ does not prefer either variant over the other.

To make predictions about the behavior of a ferromagnetic shape memory material in the case of finite anisotropy, one is faced with the task of minimizing the full energy of micromagnetics (including magnetostriction, cf. Brown [7]),

$$\int_\Omega \{\varphi(\mathbf{E}(\mathbf{x}),\mathbf{m}(\mathbf{x})) - \mathbf{h}\cdot\mathbf{m}(\mathbf{x}) - \boldsymbol{\sigma}\cdot\mathbf{E}(\mathbf{x})\}\,d\mathbf{x} + \frac{1}{8\pi}\int_{\mathbf{R}^3}|\nabla\varsigma_m|^2 d\mathbf{x} \tag{3.1}$$

Here φ is the anisotropy energy. Only the geometrically linear case is shown (this might be too special for Ni_2MnGa). Furthermore, exchange and strain-gradient terms are missing from Eq. (3.1), and therefore it is valid for large bodies. But, even if φ were known for Ni_2MnGa, which it surely is not, the minimization of (3.1) is an exceedingly difficult numerical problem, and we know no examples in the literature of the blind minimization of (3.1) for any material with appreciable mangetostriction. The main problem is the necessity of resolving complex domain structures including magnetic and structural domains.

To make progress, we are therefore led to adopt a special domain structure on observational grounds and to use (3.1) to restrict its structure. We have carried out magnetic force microscopy (MFM) studies of the (100) surface of an Ni_2MnGa specimen under no applied field or stress. A typical observation is shown in Fig. 4. These observations reveal a hierarchical domain structure of herringbone patterns, with clear observations of magnetic domains within a variant of martensite. The absence of topography is also consistent with the variants observed in Fig. 3.

How could hierarchical patterns be produced, say in the experiment shown in Fig. 1? On the top of Fig. 5 is shown a pattern predicted by the constrained theory, with an alternating series of twinned variants 1 and 2. Fig. 5 is drawn using the measured lattice parameters of Ni_2MnGa, so the 'dots' shown there can be considered as proportional to atomic positions and the easy axes are accurately shown. We imagine now increasing the field in the vertical direction, so as to favor variant 2, but we consider the possibility that $\mathbf{m}_1$ begins to rotate. A slight rotation of $\mathbf{m}_1$ through an angle θ causes a change of $O(\theta)$ in the term $-\mathbf{h}\cdot\mathbf{m}$, but only a change of $O(\theta^2)$ in the anisotropy energy (because it starts from a minimum). Hence it is plausible that $\mathbf{m}(\mathbf{x})$ rotates away from $\mathbf{m}_1$ at least a little.

The last term in (3.1) (the demagnetization energy) is nonlocal and depends on the shape of the body. It receives contributions from two sources: $\operatorname{div}\mathbf{m}$ wherever $\mathbf{m}$ is smooth, and $[[\mathbf{m}]]\cdot\mathbf{n}$ at interfaces. It is also affected by fineness, analogous to the way that the bulk elastic energy in the austenite/martensite interface can be decreased to zero by refining the twins (at the expense, of course, of interfacial energy). That is, if a fine laminate of magnetic domains $\mathbf{m}^+, \mathbf{m}^-, \mathbf{m}^+, \mathbf{m}^-,\ldots$ meets the magnetization $\mathbf{m}_2$ at an interface with normal $\mathbf{n}$, as proposed in Fig. 5b, then the demagnetization energy can be reduced to zero by refinement if

$$(\langle\mathbf{m}\rangle - \mathbf{m}_2)\cdot\mathbf{n} = ((\lambda\mathbf{m}^+ + (1-\lambda)\mathbf{m}^-) - \mathbf{m}_2)\cdot\mathbf{n} = 0, \tag{3.2}$$

where λ is the volume fraction of $+/-$ domains.

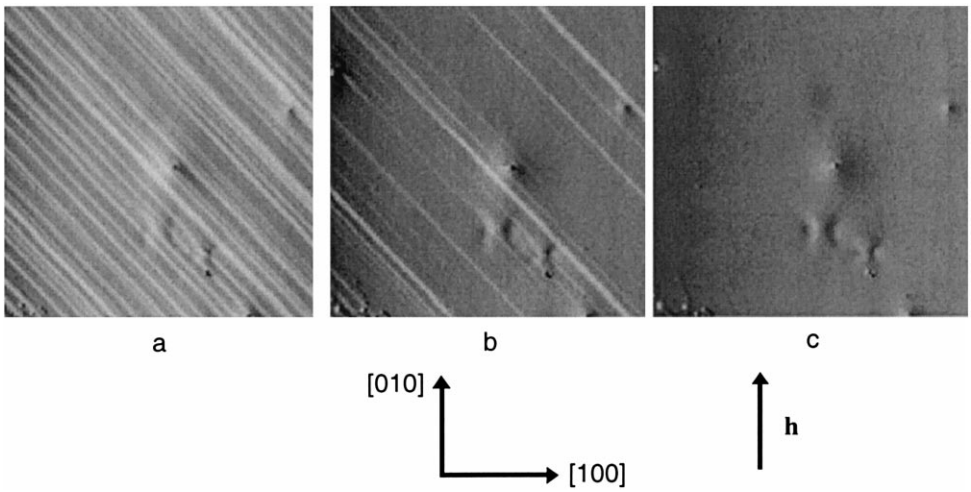

Fig. 3. Observations of microstructure at increasing field in the test shown in Fig. 2: (a) $\mathbf{h} = 6000$ Oe; (b) $\mathbf{h} = -10\,000$ Oe; (c) $\mathbf{h} = 12\,000$ Oe. For each picture the field of view is 500 μm.

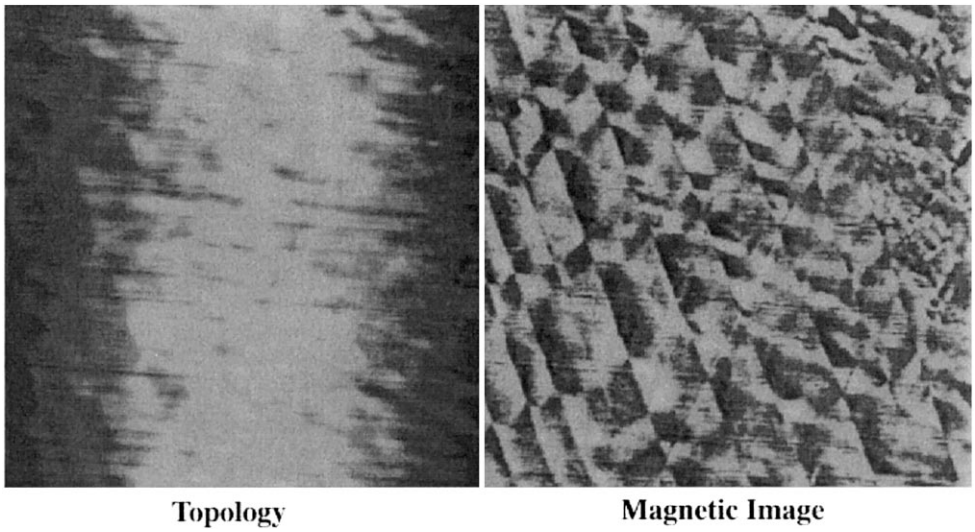

Fig. 4. MFM images of (100) surface of Ni_2MnGa. Left: topography. Right: magnetic image. Field of view is 50 μm.

Our proposed mechanism is shown in Fig. 5, arrived at in collaboration with R.V. Kohn. Since **h** is vertical, there is no tendency for $\mathbf{m}_2$ to rotate (but see the remark below). Let $\mathbf{R}_\theta$ be a counter-clockwise rotation by θ about [001]. Define $\mathbf{m}^+ = \mathbf{R}_\theta \mathbf{m}_1$, $\mathbf{m}^- = -\mathbf{R}_{-\theta}\mathbf{m}_1$ as shown in Fig. 5b. Notice that as soon as $\mathbf{m}_1$ rotates into $\mathbf{m}^\pm$ the condition $[[\mathbf{m}]] \cdot \mathbf{n} = 0$ is no longer satisfied at the twin boundaries. Thus, there is a restoring force that tries to prevent rotation based not on anisotropy energy, but instead based on demagnetization energy. Eq. (3.2) can be satisfied by choosing the specific relation $\lambda(\theta)$ that is shown in the inset of Fig. 5.

In summary, the proposed domain structure has zero 'macroscopic' demagnetization energy, and also has the feature that, by the symmetry of φ, the anisotropy energy is the same in each subdomain, so that each is equally preferred by anisotropy energy. It also has another interesting feature relating to magnetostriction of a single variant of martensite. When the magnetization within a martensitic band rotates, there is also a small magnetostriction of that variant arising again from φ. It can be shown, based only on the symmetries of φ, that the strains produced by $\mathbf{m}^\pm$ in Fig. 5b are exactly compatible across the horizontal interfaces. However, the macroscopic strain there produced by the $+/-$ domains is not compatible with the neighboring martensite band (variant 2). This is likely to lead to subdivision of both variants of martensite somewhat like the picture in Fig. 4. Since as yet we do not even know the sign of the ordinary magnetostriction of a single variant of martensite, we hesitate to make further refinements of Fig. 5. Future MFM studies of crystals under applied stress and applied field should help to support or refute the proposed domain structure shown in Fig. 5.

Acknowledgements

This research was supported by ONR-DARPA (for RDJ and RT, N00014-95-1-1145 and -91-J4034 and for MW N00014-95-1-1071 and -93-10506). The work also

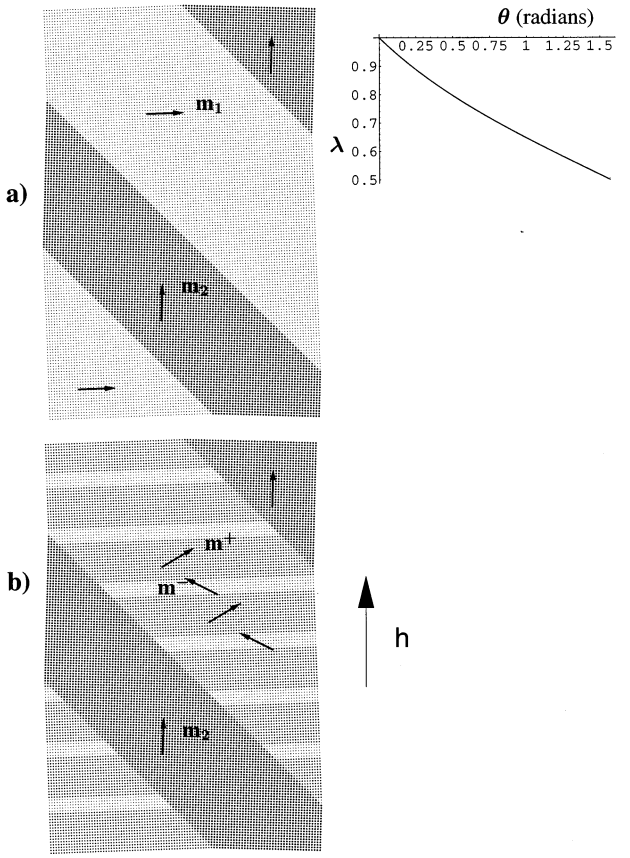

Fig. 5. Mechanism for magnetization rotation. Orientation as in Fig. 3. Inset: volume fraction λ versus angle θ of rotation that makes the macroscopic demagnetization energy vanish.

benefited from support by AFOSR/MURI F49620-98-1-0433, ARO DA/DAAG55-98-10335 and NSF DMS-9505077). We are pleased to acknowledge helpful discussions with Robert V. Kohn.

References

[1] R.D. James, M. Wuttig, Phil. Mag. A 77 (1998) 1273.
[2] R. Tickle, R.D. James, T. Shield, M. Wuttig, V.V. Kokorin, IEEE Trans. Mag., in press.
[3] A.E. Clark, B.F. DeSavage, R.M. Bozarth, Anomalous thermal expansion and magnetostriction of single-crystal dysprosium, Phys Rev. 138 (1965) A216.
[4] A.E. Clark, H.S. Belson, Phys. Rev. B 5 (1972) 3642.
[5] A.E. Clark, Ferromagnetic Materials Vol I (ea. E.P. Wolhfarth), Chapter 7. North-Holland (1980).
[6] A. DeSimone, R.D. James, A constrained theory of magnetostriction, preprint.
[7] W.F. Brown, Jr. Magnetoelastic Interactions, in: C. Truesdell (Ed.), Springer Tracts in Natural Philosophy, Vol. 9, Springer-Verlag, Berlin, 1966.